

Effects on Impurities by Boronization in REPUTE-1 RFP

Shunjiro SHINOHARA*[‡], Ken-ichi YAMAGISHI and Hiroshi TOYAMA

*Department of Physics, Faculty of Science, University of Tokyo,
Bunkyo-ku, Tokyo 113*

(Received April 7, 1994)

The effects of boronization on impurities, using a boron-trimethyl gas combined with helium glow discharge, are investigated in a reversed field pinch (RFP) device. After boronization, total pressure and partial ones of hydrogen and water decrease with the smaller pressure rise of hydrocarbons. From the surface analysis, we find the production of boron/carbon mixed layers (~40 nm thick) with metal impurities. With this conditioning, we can suppress the large increase in the plasma density. The ohmic and radiated powers in addition to impurity line intensities (especially near the plasma edge) decrease. Radial profile of soft X-ray intensity, which is higher than that before conditioning, shows somewhat broadening. The main discharges using this gas as a simple conditioning can cause the similar effects on plasma behavior.

[plasma, RFP, boronization, conditioning, radiation loss, impurity, soft X-ray, RGA, surface analysis]

§1. Introduction

Plasma-wall interaction¹⁾ is a critical important issue to be studied in order to reduce the impurity contents, which determine the radiated power loss and dilution of fuel particles as well as the confinement properties in the high temperature plasmas. In a Reversed Field Pinch (RFP) device,²⁾ which has greater current density and wall power loading than a tokamak, good plasma performance cannot be expected with the increase in the electron temperature in the near future, unless we proceed to studies on wall conditioning and wall/limiter materials.

As for wall conditioning, a glow discharge cleaning and carbonization³⁻⁵⁾ has been carried out in RFP. Recently, boronization (first boron-trimethyl $\text{-B(CH}_3\text{)}_3\text{-}$ gas⁶⁾ then B_4C rod⁷⁾ were used) has been tried to see the effects on the plasma performance. Boron coating seems to be promising because of the lower Z value compared with the carbon coating, in addition to the expectation of the oxygen reduction. However, the analyses of the produced

layer, residual gas and impurities after boronization have been reported in refs. 6 and 7 to a small extent, in spite of the great importance of the estimation of conditioning effects on plasmas.

Here, we investigate in more detail the effects of boronization, using the $\text{B(CH}_3\text{)}_3$ gas, on impurities in the reversed field pinch (RFP) device, REPUTE-1.⁸⁾ In that, conditioning procedure has been improved compared with the previous one,⁶⁾ and the sample surface, residual gas and plasma performance including impurity line intensities are successively studied. First, the analyses of the produced layer and residual gas are presented after describing the wall conditioning in §2. Next, §3 deals with the plasma performance emphasizing the impurity intensities. For comparison, plasma main discharges using the $\text{B(CH}_3\text{)}_3$ gas as a simple conditioning technique (without any glow discharges) are also tried and compared in §4 to see the effects on plasma performance and impurities. Finally, conclusions are presented in §5.

§2. Surface and Residual Gas Analyses

We briefly describe the wall conditioning performed in this experiment. The total pressure P_t (direct reading from the pirani gauge)

* Present Address: Interdisciplinary Graduate School of Engineering Sciences, Kyushu University, Kasuga 816.

† shinoigh@mbox.nc.kyushu-u.ac.jp

in the He glow discharges for two hours each, just before and after boronization, is 5–15 mTorr with an anode voltage $V_A=350\text{--}450\text{ V}$ and an anode current $I_A=1.5\text{ A}$, which corresponds to $21\ \mu\text{A}/\text{cm}^2$. Anode head has a 25 mm diameter in spheric shape, made of Mo, at a toroidal location ϕ of 30° . Current return point (earth) is located on $\phi=230^\circ$ and a gas feeding on $\phi=190^\circ$. This procedure of He glow is expected to reduce the impurity contents⁵⁾ as well as to have the lower recycling rate of hydrogen than that without He glow discharge after boronization: boron/carbon mixed layers absorb plenty of hydrogen,⁶⁾ which cause the higher plasma density. As for the boronization, $P_t=100\text{--}150\text{ mTorr}$, $V_A=400\text{--}450\text{ V}$ and $I_A=1.5\text{ A}$ for eight hours. The working $\text{B}(\text{CH}_3)_3$ gas, less toxic than diborane $\text{-B}_2\text{H}_6\text{-}$ gas,⁹⁾ is pumped with a small rate of a few 1/s to save the consumption of the gas.

Summing up, the improved and/or changed wall treatment compared with the previous one⁶⁾ (the first boronization in RFP machines) are the followings: (i) increase in the concentration of $\text{B}(\text{CH}_3)_3$ gas, diluted by He gas, from 11% to 22% for the purpose of accelerating the deposition rate of boron/carbon layers, with the higher value of P_t by a few times due to the easier production of the plasma, (ii) liner wall temperature of 120°C from room temperature throughout the conditioning (reducing the hydrogen content and a harder adherent coating can be expected¹⁾), (iii) discharge time (boronization) of eight hours from four to increase the coated layer thickness, (iv) additional He glow discharges before and after boronization, two hours each, for the sake of reducing hydrogen content and preconditioning.

After this conditioning, total pressure and partial ones of hydrogen and water decrease by a factor of ≤ 2 by a residual gas analysis (RGA) ($\phi=30^\circ$ and 230°). Helium partial pressure increases due to the He glow discharge. After the main H_2 discharges, the total pressure decreases with time for more than 10 hours (the minimum total pressure decreases by $\sim 30\%$ with remaining dominant components of hydrogen and water), whereas only about 3 hours before this conditioning.

Although partial pressures of hydrocarbons increase drastically during boronization (low mass numbers m (less than 20), intermediate m of 36–45 and 50–58 and high m of 65–71 and 79–82), whose result is nearly the same with ref. 6, these hydrocarbons fade after He glow discharge except for low m , $m=40\text{--}44$ and 79–82. After main discharges with H_2 gas, almost all remained hydrocarbons decrease shot by shot.

From the analysis of a Si wafer sample (not heated), $10\text{ mm} \times 10\text{ mm}$ with 0.5 mm thickness, exposed to the plasma edge (minor plasma radius $a=22\text{ cm}$) during boronization ($\phi=230^\circ$), using an Auger Electron Spectroscopy (AES) method (Auger Microprobe, JEOL Ltd., JAMP-10S), we find the production of the boron/carbon mixed layers; The concentration of carbon is larger than that of boron, and the metal impurities such as Ni (most dominant component), Fe and Cr are also found, all of which come from a liner component made of Inconel 625. The thickness of the layer estimated from AES with an Ar ion beam etching is $\sim 42\text{ nm}$. This coated layer is thinner than the estimated value by several times. This may be due to the (global) non-uniformity of the thickness along the toroidal direction,¹⁰⁾ lower flow rate, higher working gas pressure and lower deposition efficiency etc.

The surface profilometer (Tencor Instruments, α Step 200) shows this thickness is $\sim 38\text{ nm}$, which is consistent with AES result, and also shows the nearly flat plane with several nm undulation in $50\ \mu\text{m}$ length along the surface and $\leq 1\text{ nm}$ in $1\ \mu\text{m}$. According to a picture (Fig. 1) taken by the scanning electron microscope (SEM) (Topcon Corp., ABT-32 and JEOL Ltd., JAMP-10S), there are several peaks within the region of $2\ \mu\text{m} \times 2\ \mu\text{m}$, which have circle shapes of $\leq 0.4\ \mu\text{m}$ diameter. These show that the nearly smooth plane has been produced by this conditioning. (If it is not flat at all, an influx of metal impurities, which comes from the bare liner or thinner layer parts during main discharge, may not be expected to be reduced so much.)

§3. Plasma Behavior and Impurities

Typical plasma current I_p using H_2 gas (pre-

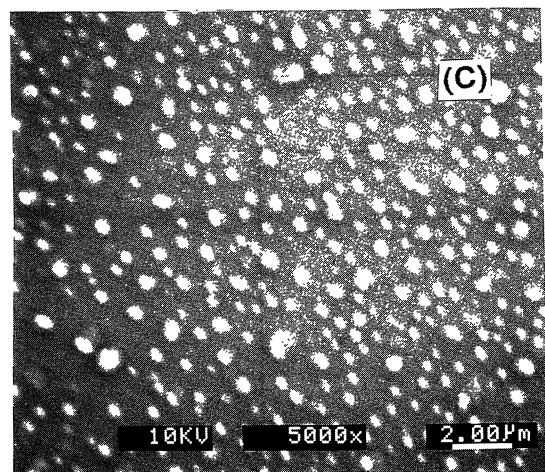
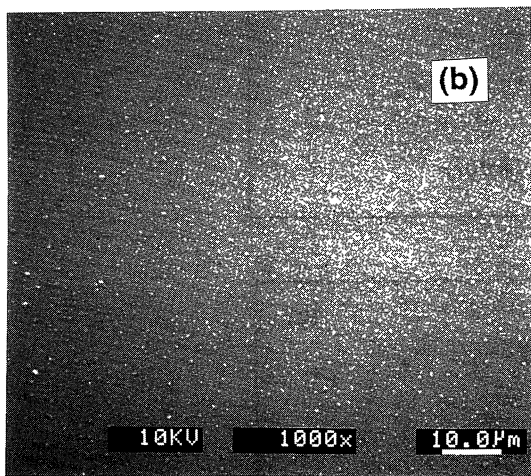
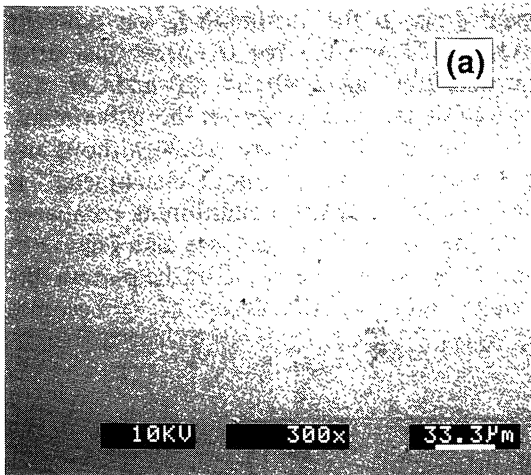


Fig. 1. SEM micrographs magnify the sample surface, which is exposed to the plasma edge during boronization, by 300 (a), 1000 (b) and 5000 times (c). Scales and accelerating voltage of 10 kV are also shown.

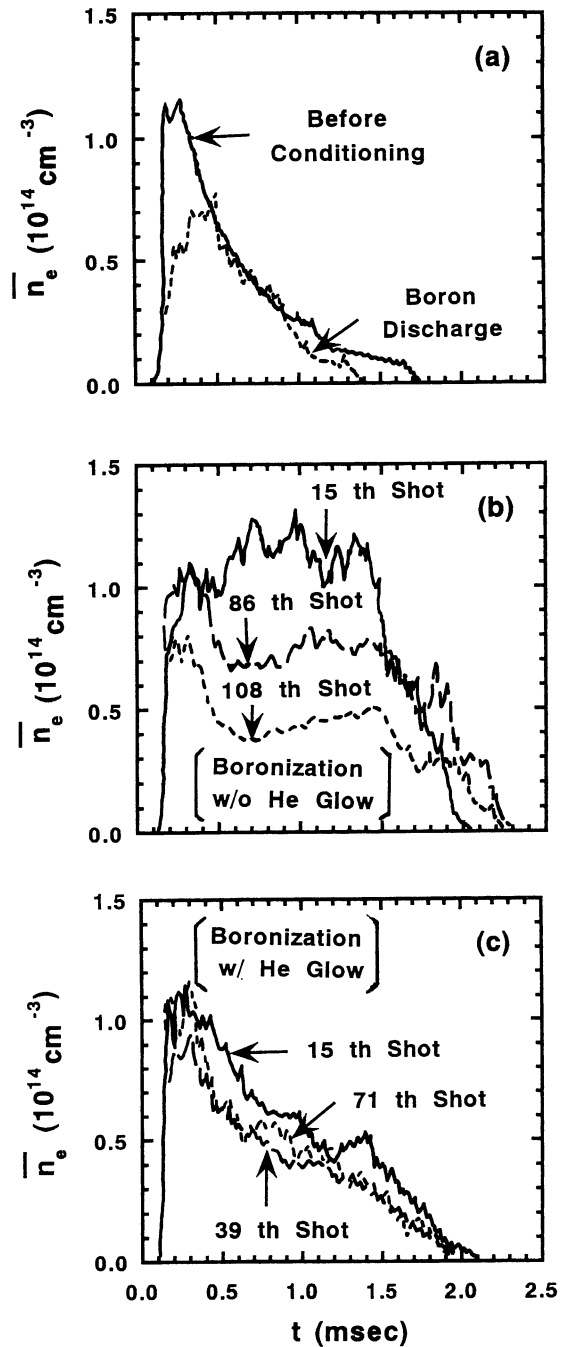


Fig. 2. Time evolutions of mean plasma density \bar{n}_e before conditioning (bold line) and during boron discharge (dotted line) (a), after boronization without (b) and with (c) He glow. Shot numbers after boronization are also shown.

filling) for the comparative study is ~ 200 kA. By the use of the combined He glow discharge and wall temperature of 120°C after boronization, we can not find the uncontrollable large increase in the mean plasma density \bar{n}_e near the time of the maximum I_p normalized by the filling pressure. This is shown in Fig. 2(c), comparing with the previous boronization without He glow⁶⁾ in Fig. 2(b) (\bar{n}_{ef} : calculated density assuming a complete ionization of the filling

gas): \bar{n}_e/\bar{n}_{ef} at the maximum I_p was typically ~ 1.8 , 0.55 and 0.3 for the cases just after boronization, after 50 and 120 main H_2 discharge shots, respectively. In this experiment, this value is ~ 0.35 where ~ 0.24 without any conditioning. "No pumpout phenomena" is also alleviated by this conditioning compared with the no He glow case (see also Figs. 2(b) and 2(c)). At the later stage of the plasma discharge duration, the decay of I_p becomes

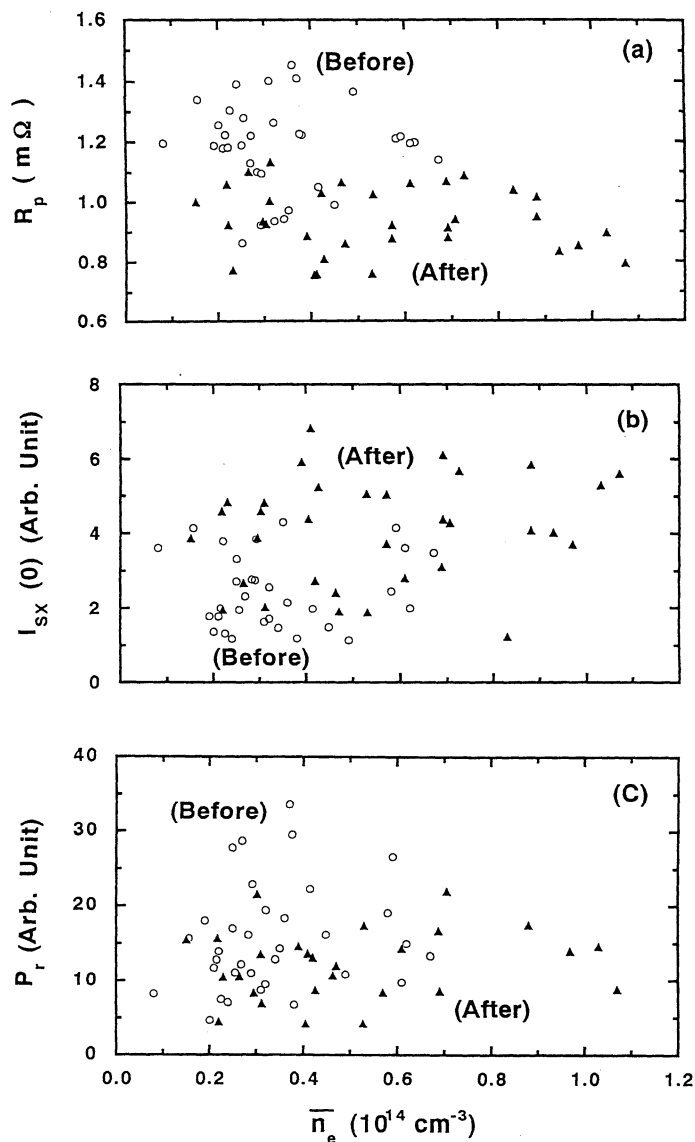


Fig. 3. Plasma resistance R_p (a), central soft X-ray intensity $I_{sx}(0)$ (b) and radiated power P_r (c) vs. mean plasma density \bar{n}_e . Here, open circles and closed triangles show cases before and after boronization, respectively.

slower with a reduction of the V_1 (one-turn loop voltage) increase, which is the same result in ref. 6.

Figure 3 shows the plasma resistance R_p ($=I_p/V_1$), central soft X-ray intensity $I_{sx}(0)$ ($\phi=90^\circ$)¹¹ and radiated power P_r by a bolometer (nearly central chord) ($\phi=150^\circ$)⁶ as a function of the mean plasma density \bar{n}_e , taken at the time of the peak plasma current. By the boronization, plasma resistance R_p , hence an ohmic power P_Ω , and P_r decrease appreciably, whereas the ratio of P_r to P_Ω does not change very much. On the other hand, soft X-ray intensities increase (on all (11 ch) chord radii r from $-0.7a$ to $0.7a$). These results suggest the lower Z_{eff} (effective charge) and higher electron temperature after the conditioning; Decreases in impurity line intensities with the same electron density, which will be described after, as well as a decrease in P_r imply mostly the lower Z_{eff} . Based on the relation that I_{sx} is roughly proportional to $Z_{eff} n_e^2 T_e^{3-3.5}$ for $T_e=50-300$ eV (bremsstrahlung) in this system, the increase in I_{sx} with the same \bar{n}_e may come from the electron temperature rise. The decrease in R_p , which is proportional to $Z_{eff}/T_e^{1.5}$ also supports the above conclusion. This result is different from the previous one⁶ that the radiated power was reduced while the electron temperature did not change appreciably (R_p decreased by only $\sim 10\%$ and I_{sx} decreased somewhat due to mainly a reduction of Z_{eff}).

As for the soft X-ray intensity profiles, somewhat broader profiles are observed: at the outer plasma region ($|r| > 8$ cm), normalized intensity $I_{sx}/I_{sx}(0)$ increases a little. Full widths at half maximum and at a quarter maximum are from ~ 15.9 cm to ~ 16.9 cm and from ~ 21.9 cm to ~ 24 cm, respectively. By boronization, the upper operating density without deleterious effects becomes higher as shown in Fig. 3. Without the conditioning, R_p and P_r are higher when $\bar{n}_e > 0.8 \times 10^{14}$ cm⁻³ and it is difficult to enter such high density regime. This condition to have this higher plasma density contributes to the increase in the energy confinement τ_E , i.e., τ_E increase with \bar{n}_e .^{2,5} It also may compensate for the beta poloidal decline, which will be a problem in the larger current regime in the near future.²

Next, we report the changes (mostly decreases) of impurity line intensities measured by a visible monochromator ($\phi=90^\circ$).¹² Figure 4 shows the comparison of the various line intensities before and after the conditioning of boronization combined with He glow discharge described before. Here, averaged values over several plasma shots (each signal) at the time of I_p peak are taken and are normalized to be unity for no conditioning case. Note that line intensities are measured for various plasma density and the average value of \bar{n}_e is higher after the boronization for this data set (and impurity line intensity is not so sensitive

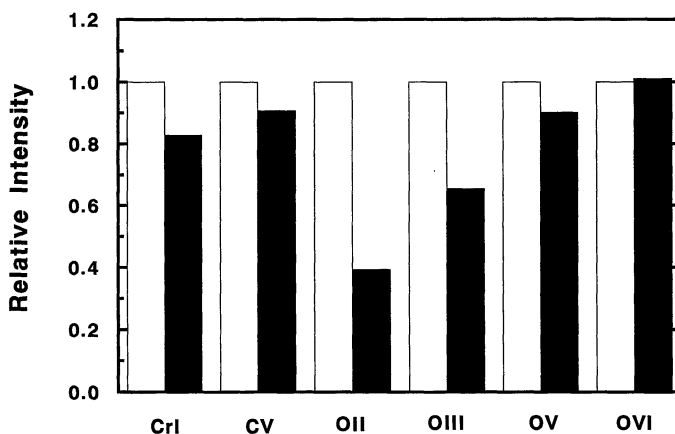


Fig. 4. Comparison of the various impurity line intensities before (open bars) and after (closed bars) boronization.

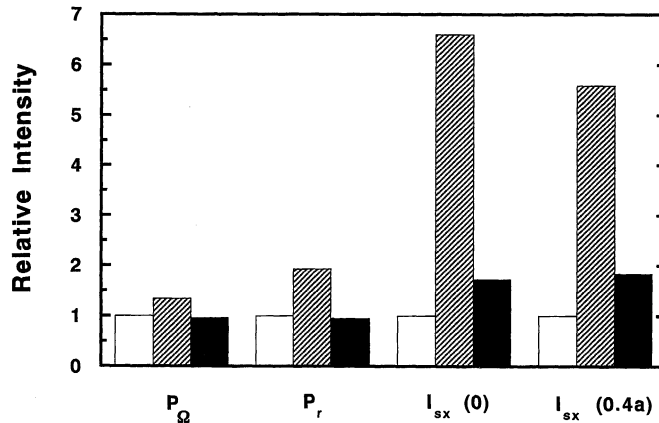


Fig. 5. Comparison of the ohmic and radiated powers, P_{Ω} and P_r , soft X-ray intensities at the central and intermediate regions, $I_{sx}(0)$ and $I_{sx}(0.4a)$, before (open bars), during (shaded bars) and after (closed bars) main $B(CH_3)_3$ gas discharges.

to \bar{n}_e experimentally). Therefore, the impurity reduction rate is more (by a factor of ≤ 1.5) if the respective impurity intensity is normalized by \bar{n}_e .

The observed salient feature is that the reduction rate of oxygen intensity is larger at the lower ionization potential than the higher one: the largest for OII (wavelength=313.5 nm and ionization potential=35.1 eV) line, next for OIII (268.6 nm, 54.9 eV) and the third for OV (278.1 nm, 113.9 eV), whereas OVI (343.4 nm, 138.1 eV) intensity changes little. Emitted region moves in from the plasma edge (OII line, lower charged state) to the plasma core (OVI, higher charged state). In addition, CrI (427.5 nm, 6.8 eV) intensity, which reflects the plasma-wall interaction (boundary), decreases. These results show that the conditioning affects the impurity line intensity more clearly at the plasma boundary (CrI and OII line intensities) than the core and also the reduction effect of OV is larger than the previous one,⁶⁾ in which OV intensity did not decrease. Although there are no data on the uniformity (around the toroidal direction) of impurity line intensities emitted near the plasma edge, the plasma-wall interaction may be stronger at the large error region in RFPs, e.g., plasma edge near the shell gap ($\phi=0^\circ$ and 180°), and near the low toroidal field region (larger field ripple) of $\phi=(1+2n)$

$\times 3.3^\circ$ (n : integer) at the outer equator (monochromator ($\phi=90^\circ$) is also located on this region).

The reason why line intensities with the higher charged states such as OV and OVI (which emit from between the inner and the central plasma regions) is not changed very much compared with the lower charged state, may be considered as follows; As the central electron temperature T_e (≤ 100 eV) is smaller than the ionization potential for these lines, the increase in T_e (and/or local increase in plasma density n_e) cancels the lesser content of oxygen density due to the conditioning. There is also another possibility that the oxygen density is not reduced so much in the plasma core. As is described before, slower I_p decay and lower V_1 increase are observed near the end of discharge duration. In this phase, the smaller increase in impurity line intensities (especially lower charged states) compared with the case before boronization is also found.

The CV (278.1 nm, 392.1 eV) intensity decreases little and is nearly constant during the successive discharge shots. On the contrary, the BV (282.5 nm, 259.4 eV) intensity increases drastically and decreases shot by shot (e-folding shot is ~ 50). These improved plasma performance mentioned above gradually fades after a few hundreds of plasma discharge shots.

Although recycling of hydrogen is reduced in the He glow discharge case,⁵⁾ an improvement of plasma behavior is better in this experiment. Comparing with the previous boronization case,⁶⁾ combined effect of He glow discharge and wall temperature of 120°C in addition to boronization, causes the lower recycling of hydrogen and enhances the better plasma performance such as more reductions of plasma resistivity and impurity intensities. This indicates the higher electron temperature, in contrast to little change in the previous case,⁶⁾ as is also shown by the increase in soft X-ray intensity.

Although coated layer is a mixture of boron and carbon in this boronization, results from the RGA analysis and plasma behavior exhibit the different feature compared with the carbonization case.⁵⁾ In this case, total pressure and partial ones of hydrocarbons and hydrogen increased (not decreased). A rise of \bar{n}_e/\bar{n}_{ef} was found to be less than that after boronization alone.⁶⁾ This shows that the boron layer can absorb hydrogen more than the carbon layer (~ 0.4 hydrogen/carbon atom¹⁾) at room temperature (wall). However, we can easily lower the hydrogen concentration in the B/C layer by the main H₂ discharge (or He glow/wall temperature rise) in contrast with the carbonization. Reductions of plasma resistance and impurity line radiation are common features between carbonization and boronization (with and without He glow/wall temperature rise), regardless of the different lowering rates. Two hours He glow discharge after boronization may exceed the helium ion dose required for wall pumping of H₂ gas, i.e., conditioning effect on hydrogen recycling (at least this He glow satisfies the condition in B₂H₆ gas case¹³⁾).

§4. Main Discharges Using Boron-Trimethyl Gas

Here, the characteristics of the plasma main discharges (33 successive shots for $I_p \sim 200$ kA), using the B(CH₃)₃ gas (22%) diluted by He gas directly as a fuel gas, for the simple boron/carbon coating (without any glow discharges) is described. During the main boron discharges, we observe the drastic increases in plasma parameters such as R_p , P_Ω , P_r , impurity lines (oxygen and carbon) by a factor of 1–2, and

HeI (468.6 nm, 24.6 eV), HeII (388.9 nm, 54.4 eV) lines as well as all channels of soft X-ray intensities by a factor of >4 . The \bar{n}_e/\bar{n}_{ef} value (\bar{n}_{ef} is calculated on the condition that the filling gas of He or B(CH₃)₃ is fully ionized) decreases by a factor of ~ 3 with the nearly same \bar{n}_e (if \bar{n}_{ef} is taken from only hydrogen component, \bar{n}_e/\bar{n}_{ef} increases by ~ 1.3 times). Typical time evolution of mean plasma density \bar{n}_e is shown in Fig. 2(a), which represents a different behavior compared with the case without any conditioning.

After this simple conditioning, total and partial oxygen pressures decrease by a factor of ≤ 1.5 (partial hydrogen pressure increases by ≤ 2) from RGA, and the better plasma performance is found, which is similar to the results described in §3. Figure 5 shows the changes of plasma behavior before, during and after main B(CH₃)₃ gas discharges at the time of the plasma current peak. The ohmic and radiated powers, P_Ω and P_r , decrease after this conditioning. On the contrary, the soft X-ray intensities at the central and intermediate regions, $I_{sx}(0)$ and $I_{sx}(0.4a)$ increase, which is supposed to be due to increase in the electron temperature as the lowering of impurities is observed (the same discussion in §3); CrI and lower states of oxygen intensities decrease. The HeI and HeII intensities, which increase by a few times after boron discharge, decrease shot by shot. Somewhat broadening of the soft X-ray profile is also found. The \bar{n}_e/\bar{n}_{ef} value increase by ≤ 1.3 with the nearly same \bar{n}_e due to the coating layer which contains higher hydrogen density. These better plasma behaviors gradually fades after several tens of plasma discharge shots.

§5. Conclusions

The effects of boronization on impurities, using the B(CH₃)₃ gas diluted by He gas, combined with He glow are investigated intensively in the RFP device, REPUTE-1. After the conditioning, total pressure and partial ones of hydrogen and water decrease with the smaller pressure rise of hydrocarbons than the previous result.⁶⁾ The surface deposited on the Si sample wafer is analyzed by AES, SEM and the surface profilometer. The thickness of the layers, which are made of boron/carbon

mixed with metal impurities such as Ni, Fe and Cr, is ~ 40 nm,

Due to the He glow discharge and/or wall temperature of 120°C after boronization, we can suppress the large increase in the plasma density at the flat I_p phase: \bar{n}_e/\bar{n}_{ef} can be lowered. The ohmic and radiated powers decrease, and also the impurity line intensities of OII, OIII, OV, CrI and CV decrease (observed reduction rate is higher near the plasma edge), whereas the BV intensity transiently increases. Radial profile of soft X-ray intensity, which is higher than before boronization, shows somewhat broadening. These results show the significant reduction of impurities and better plasma performance due to the conditioning. The main discharges using the $\text{B}(\text{CH}_3)_3$ gas as a simple conditioning cause similar effects on plasma parameters.

Acknowledgement

The authors are grateful to T. Oikawa and the REPUTE-1 group for operating this device. This work has been partly supported by a Grant-in-Aid for Scientific Research from the Ministry of Education, Science and Culture.

References

- 1) P. C. Stangeby and G. M. McCracken: Nucl. Fusion **30** (1990) 1225.
- 2) H. A. B. Bodin: Nucl. Fusion **30** (1990) 1717.
- 3) K. F. Schoenberg, G. A. Wurden, P. G. Weber, J. C. Ingraham, C. P. Munson, D. A. Baker, C. J. Buchenauer, L. C. Burkhardt, T. E. Cayton, J. N. DiMarco, J. N. Downing, R. M. Erickson, P. R. Forman, A. Haberstick, R. B. Howell, F. C. Jahoda, R. S. Massey, G. Miller, R. W. Moses, Jr., R. A. Nebel, J. A. Phillips, M. M. Pickrell, A. E. Schofield, R. G. Watt, D. M. Weldon and K. A. Werley: *Proc. 11th Int. Conf., Kyoto, 1986* (Plasma Physics and Controlled Nuclear Fusion Research 1986) (IAEA, Vienna, 1987) Vol. 2, p. 423.
- 4) G. L. Jackson, T. S. Carlstrom, B. Curwen, R. R. Goforth, D. W. Graumann, T. Tamano and P. L. Taylor: J. Nucl. Mater. **145-147** (1987) 470.
- 5) S. Shinohara, K. Yamagishi, S. Ohdachi, A. Ejiri, K. Mayanagi, Y. Shimazu and K. Miyamoto: Plasma Phys. Control. Fusion **34** (1992) 627.
- 6) S. Shinohara, K. Yamagishi, S. Ohdachi, A. Ejiri, H. Toyama and K. Miyamoto: J. Phys. Soc. Jpn. **61** (1992) 3030.
- 7) D. J. Den Hartog, M. Cekic, G. Fiksel, S. A. Hokin, R. D. Kendrick, S. C. Prager and M. R. Stoneking: J. Nucl. Mater. **200** (1993) 177.
- 8) N. Asakura, T. Fujita, K. Hattori, N. Inoue, S. Ishida, Y. Kamada, S. Matsuzuka, K. Miyamoto, J. Morikawa, Y. Nagayama, H. Nihei, S. Shinohara, H. Toyama, Y. Ueda, K. Yamagishi and Z. Yoshida: Plasma Phys. Control. Fusion **28** (1986) 805.
- 9) H. G. Esser, V. Philipps, H. B. Reimer, P. Wienhold and the TEXTOR Team: Nucl. Fusion **32** (1992) 278.
- 10) H. Sugai, M. Yamage, Y. Hikosaka, T. Nakano and H. Toyoda: J. Nucl. Mater. **200** (1993) 403.
- 11) N. Asakura, Y. Nagayama, S. Shinohara, H. Toyama, K. Miyamoto and N. Inoue: Nucl. Fusion **29** (1989) 893.
- 12) A. Fujisawa, H. Ji, K. Yamagishi, S. Shinohara, H. Toyama and K. Miyamoto: Nucl. Fusion **31** (1991) 1443.
- 13) M. Yamage, T. Ejima, T. Toyoda and H. Sugai: J. Nucl. Mater. **196-198** (1992) 618.